JACS
JOURNAL OF THE AMERICAN CHEMICAL SOCIETY

Article

pubs.acs.org/JACS

In Vitro Reversible Translation Control Using γPNA Probes

Taylor D. Canady,[†,§] Cheryl A. Telmer,[‡,§] Stanley N. Oyaghire,[†,§] Bruce A. Armitage,[*,†,§] and Marcel P. Bruchez[*,†,‡,§]

[†]Department of Chemistry, [‡]Department of Biological Sciences, and [§]Center for Nucleic Acids Science and Technology, Carnegie Mellon University, 4400 Fifth Avenue, Pittsburgh, Pennsylvania 15213, United States

Supporting Information

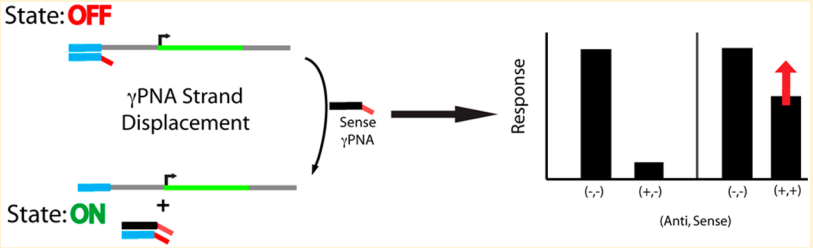

ABSTRACT: On-demand regulation of gene expression in living cells is a central goal of chemical biology and antisense therapeutic development. While significant advances have allowed regulatory modulation through inserted genetic elements, on-demand control of the expression/translation state of a given native gene by complementary sequence interactions remains a technical challenge. Toward this objective, we demonstrate the reversible suppression of a luciferase gene in cell-free translation using Watson−Crick base pairing between the mRNA and a complementary γ-modified peptide nucleic acid (γPNA) sequence with a noncomplementary toehold. Exploiting the favorable thermodynamics of γPNA−γPNA interactions, the antisense sequence can be removed by hybridization of a second, fully complementary γPNA, through a strand displacement reaction, allowing translation to proceed. Complementary RNA is also shown to displace the bound antisense γPNA, opening up possibilities of in vivo regulation by native gene expression.

INTRODUCTION

Methods to irreversibly interfere with gene expression (e.g., antisense targeting of mRNA) are well-known chemical biology tools and potential therapeutic strategies. Reversible regulation of gene expression offers the opportunity to perturb gene regulatory networks and signaling cascades. Through the use of a serial method of translation control, investigations related to the temporal and spatial effects of a specific transcript can be approached. Through the careful attention to chemical probe affinity and selectivity, control over protein expression is possible at the transcript level, which allows for the direct investigation at precise nodes in biochemical pathways. Importantly, achieving reversible control through the supply of an external probe can enable numerous interventions and manipulations of native genetic elements in order to assess or control downstream phenotypic effects. To this end, chemical probes can be introduced at precise time points, allowing for on-demand control of translation locally or systemically, depending on the method of probe delivery.

Synthetic translation regulation has been implemented through the utilization of various engineered mRNAs and antisense-probe manipulations. Facile examples of ligand dependent (i.e., riboswitches[1]) protein expression, sequence optimization (ribosome binding site strength[2]), and direct expression knockdown through exogenous and endogenous probe hybridization[3] have provided a way to selectively (de)-activate target transcripts. Translation regulation through a strand displacement mechanism has also been realized. For example, through the careful design of toehold-driven RNA interactions, conditional RNAi mediated knockdown has been demonstrated.[4] Furthermore, the mRNA transcript itself has been engineered to display conditional RBS sequestration, whereupon translation is driven by a small noncoding RNA displacement reaction.[5] Using this approach, Green and co-workers recently reported improved transcript designs for higher-fold GFP activation and generalized the design to detect a much larger set of small RNA targets (triggers).[6] In terms of antisense reversible regulation, Young et al. suppressed gene expression knockdown and then subsequently reactivated it by manipulating a light-sensitive antisense agent that undergoes an intramolecular strand displacement reaction.[7] This work demonstrated the feasibility of light-defined control over reporter expression where reversibility was established through application of caged antisense probes. Nevertheless, achieving light-activated translation control is limited to a relatively small sensitized area and penetrance depth, thus precluding systemic translation control (i.e., whole animal). To achieve translation control in a systemic manner, as well as limit any genetic manipulation of target transcripts, we designed a translation control system consisting of an antisense agent that inhibits

Received: May 22, 2015
Published: August 4, 2015

DOI: 10.1021/jacs.5b05351
J. Am. Chem. Soc. 2015, 137, 10268−10275

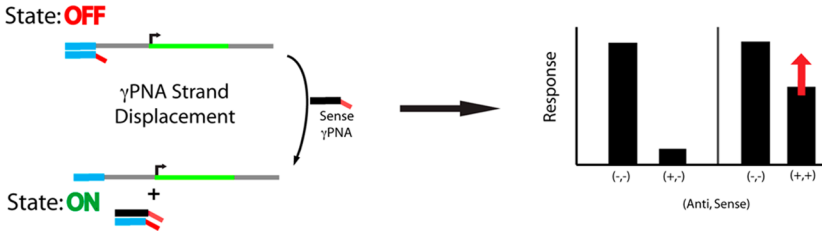

Figure 1. Reversible translational control through use of γPNA probes. State: OFF is established by the introduction of an antisense γPNA that binds to a partially cognate mRNA transcript, leaving the adjoining toehold domain free. With the introduction of sense γPNA, a subsequent γPNA–γPNA (toehold nucleation event) binding event initializes strand displacement, rendering the translation to State: ON. The subsequently altered luciferase expression can be plotted to measure the translation recovery (right illustration).

translation but can be subsequently displaced from the mRNA target by a suitable complementary sense agent.

A probe that alters translation must display the requisite affinity and specificity in order to have the desired activity without detrimental off-target effects. Peptide nucleic acids (PNA[8,9]) provide high affinity for complementary RNA targets, with biological stability owing to the unnatural backbone configuration. The ability of PNA to interfere with gene expression has been well documented,[10] with examples including modulation of transcription,[11−13] pre-mRNA splicing,[14−16] mRNA translation,[17−20] and miRNA function.[21,22] γPNA, a second generation analogue of PNA,[23] exhibits enhanced target affinity and increased water solubility compared to traditional PNA.[24] These features arise from the fact that γ-modifications that introduce an appropriate chirality to the PNA backbone induce right-handed helicity that closely resembles the structure of the γPNA when hybridized to complementary DNA/RNA, leading to enhanced target affinity. Meanwhile, the diethylene glycol (miniPEG) substituent used in the current work provides significantly improved water solubility relative to PNA.[24] γPNA has shown promising target selectivity with excellent mismatch discrimination,[24] and guanidinium-modified γPNA has been shown to inhibit translation of mRNA within living cells.[25] Moreover, γPNA–γPNA duplexes are significantly more stable than γPNA–RNA heteroduplexes, meaning our proposed approach relies on a thermodynamically favorable process.[26] Furthermore, PNA molecules are nuclease, protease, and peptidase resistant, which makes them stable in biological milieu, such as the cell lysates we used in the following in vitro translation experiments.[27] Although γPNA's stability under these conditions has not been characterized, we expect it to be similarly resistant to enzymatic degradation. Herein, we demonstrate reversible translation control mediated through a γPNA–γPNA strand displacement process.

RESULTS

Reversible translation control is achieved through two separate and fully complementary γPNA molecules. The first γPNA is required for direct mRNA target binding (antisense) which represses translation. The second (sense) γPNA derepresses translation through a γPNA–γPNA displacement interaction, mediated by a free toehold sequence on the first (antisense) γPNA strand (Figure 1).

Reversible control of translation by base-pairing requires two functioning components: (i) a sequence-selective probe that suppresses translation effectively and (ii) an agent that can relieve this suppression. Previous antisense "gene walk" investigations with PNA established two effective native mRNA target sites[18,28,29] (*i*) the 5′-terminal end of the mRNA and (*ii*) proximal to or at the Kozak initiation sequence and AUG start codon. Relative to eukaryotic translation, probe hybridization at the terminal end of the 5′-UTR is largely believed to attenuate translation by inhibiting the attachment of the 43S ribosomal preinitiation complex to the transcript and thus blocking initiation of translation.[18,29] When a probe is targeted to the Kozak/AUG region,[30] both ribosomal scanning of the 5′-UTR and subsequent translocation into the coding region are prevented.[31] The removal of the antisense block from the mRNA transcript via strand displacement from either site would release a fully functional native mRNA and allow translation to proceed.

Translation Suppression by PNA and γPNA. To begin development of the translational switch, two unmodified 15-mer PNA probes were synthesized that were designed to bind to the above-mentioned sites within a luciferase transcript. Both of the PNAs display IC_{50} values in the low nM range (Figure S1A), indicative of excellent in vitro targeting, while maintaining negligible activity toward an orthogonal 5′-UTR luciferase transcript that lacks the PNA target sites (Figure S1B). To improve target binding, analogous γPNA (γ = (*R*)-diethylene glycol, "miniPEG") oligomers were prepared. As mentioned above, γPNA has been demonstrated to exhibit favorable RNA duplex stability, while still maintaining target selectivity. Due to the higher thermodynamic stability of γPNA–RNA interactions, compared to PNA–RNA,[24] we synthesized two γPNAs (10-mer and 15-mer) targeting the 5′ terminus of the mRNA (referred to as **γPNA$_{10}$** and **γPNA$_{15}$**). For reference, the luciferase mRNA target sequence and the γPNA sequences are given in Table 1.

The antisense dose response relationship for both **γPNA$_{15}$** and **γPNA$_{10}$** probes against the luciferase reporter are presented in Figure 2A. Both probes gave low IC_{50} values (<50 nM). Furthermore, a dose of 100 nM γPNA gave >85% gene knockdown for both cases. Unexpectedly, the two γPNAs gave similar IC_{50} values despite the difference in length. Nonetheless,

Table 1. 5′-Terminal mRNA Target Sequence[a]

mRNA Target	5′-AGACCCAAGCUUUCA-3′
γPNA$_{15}$	NH_2-K-TCTGGGTTCGAAAGT-H
γPNA$_{10}$	NH_2-K-TCTGGGTTCG-H

[a]The γPNAs sequences are written from the C-terminus to the N-terminus, "K" represents lysine. The 5′-end of the mRNA transcript is hybridized with the C-terminal end of the γPNA oligonucleotide.

DOI: 10.1021/jacs.5b05351
J. Am. Chem. Soc. 2015, 137, 10268−10275

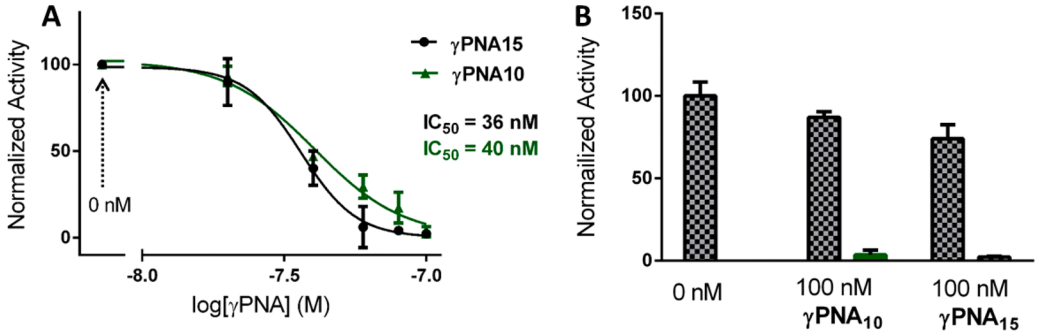

Figure 2. γPNA antisense gives effective and specific luciferase knockdown. (A) Overlay of antisense dose−response curves for both $\gamma\mathbf{PNA}_{10}$ and $\gamma\mathbf{PNA}_{15}$ (both tested at $n = 3$) tested against the luciferase mRNA (10 nM). The γPNA probe and mRNA were preannealed in a buffered solution (RRL-matching concentration of 79 mM K^+ and DEPC-treated H_20) and then placed in a 37 °C for 1 h. (B) γPNA probes against a luciferase mRNA (10 nM) that has a scrambled γPNA target site (checkered bars). $\gamma\mathbf{PNA}_{10}$ shows insignificant knockdown ($p > 0.05$) and $\gamma\mathbf{PNA}_{15}$ shows small (∼15%) but potentially significant ($p < 0.05$) luciferase knockdown. The knockdown of the perfect match luciferase is shown for $\gamma\mathbf{PNA}_{15}$ (100 nM, black bar) and $\gamma\mathbf{PNA}_{10}$ (100 nM, green bar).

the improved efficacy of the γPNAs compared to the PNA is consistent with the enhanced γPNA thermodynamic stability. In addition, by utilizing an mRNA transcript with an orthogonal 5′-UTR, we observed only slight (∼10−15%) off-target luciferase knockdown (Figure 2B), again likely due to the higher affinity trade-off. Having observed sufficient antisense knockdown for both lengths of γPNA, subsequent γPNA translational control probes were based off the shorter γPNA_{10} sequence.

Reversible Translation Suppression with γPNA. Because the 10-mer sequence is effective for translational suppression, we designed an extended γPNA probe containing the same 10-base mRNA binding domain and a contiguous 5-nucleobase toehold that is not complementary to any site on the mRNA (Figure 1). The toehold domain functions as a nucleation site that mediates the displacement of the bound antisense strand by addition of the second sense γPNA. The sense γPNA is fully complementary to antisense γPNA, leading to 5-extra base pairs (for specific sequence design see Table 2).

Table 2. Specific γPNA Sequence Used in Reversible Experiments[a]

mRNA Target	5′-AGACCCAAGC-3′
Antisense γPNA	H_2N-K-TCTGGGTTCGTGATA-H
Sense γPNA	H-AGACCCAAGCACTAT-K-NH_2

[a]Complementary toehold domains indicated in red. K = lysine.

The use of a 5-nucleobase toehold was determined by previous reports that show this to be a suitable length[32] for strand displacement reactions in DNA-based manipulations. Hence, upon the introduction of the complementary sense γPNA and through binding of the sense toehold to the complementary antisense toehold, a strand displacement reaction should free the mRNA transcript and toggle translation back ON.

To characterize the γPNA−γPNA displacement reaction, we designed a series of surface plasmon resonance (SPR) experiments to verify and quantify the displacement reaction. Unfortunately, SPR is not amenable to direct immobilization of RNA due to the harsh chip regeneration conditions (i.e., NaOH wash) needed to remove bound γPNA prior to the next injection of sample. Given this, the SPR chip is functionalized with an immobilized biotinylated-DNA target, where the DNA sequence matches the target mRNA probe binding domain. Antisense γPNA is then injected (20 nM) into the flow cell to allow the target DNA-antisense γPNA hybridization reaction to occur (Figure 3). Subsequently, a short buffer wash is used to remove any unbound antisense γPNA, and then a titrated concentration (0−200 nM) of sense γPNA is flowed over the chip to allow for the γPNA−γPNA displacement reaction. A successful displacement reaction causes an overall loss of mass on the chip and generates a discernible dissociation curve on the SPR sensorgram (Figure 3). The percent displacement should increase as a function of sense concentration.

Figure 4 demonstrates that the displacement experiment functions as illustrated in Figure 3. Loading of the antisense γPNA results in strong increase in signal, while subsequent addition of sense γPNA decreases the signal in a dose-dependent manner. Interestingly, only ca. 50% of the antisense γPNA could be displaced, based on the decrease in the observed response units. However, subsequent control experiments revealed that high (i.e., >100 nM) concentrations of sense γPNA led to nonspecific binding to the SPR chip, which evidently compensates for the loss in mass due to specific displacement of the antisense γPNA. (These experiments are described in detail in the Supporting Information.)

To verify that the presence of the antisense toehold was necessary for displacement, we repeated the SPR displacement reaction by considering two separate experimental toehold-control conditions. The first control removed the toehold from the antisense γPNA to test if displacement driven by the sense γPNA can still proceed without proper toehold nucleation to the γPNA-10mer sequence. Here, we found that the removal of the antisense toehold gave no measurable displacement on the SPR (Figure 4C and Figure S4A). The second control experiment utilized a longer immobilized target that completely base-pairs with the antisense γPNA toehold. When the longer target was applied, there was minimal detection of sense γPNA driven displacement (Figure 4C and Figure S4B) presumably due to sequestering the antisense toehold.

After observing γPNA-driven displacement on the SPR, in vitro translation control studies were then conducted. The initial antisense γPNA probe was preannealed to the target

DOI: 10.1021/jacs.5b05351
J. Am. Chem. Soc. 2015, 137, 10268−10275

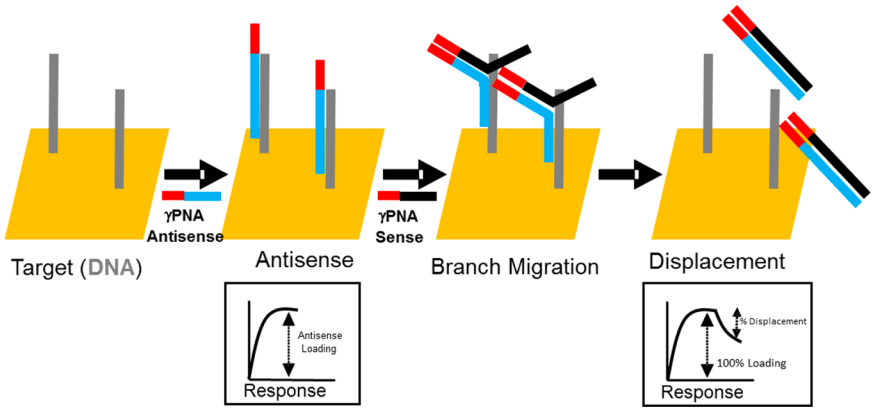

Figure 3. Surface plasmon resonance (SPR) investigation of γPNA–γPNA strand displacement. Antisense γPNA (light blue), with toehold (red), is loaded (association phase) onto the SPR chip via a hybridization reaction with the surface bound DNA (gray) capture strand. A wash step is included to remove any residual antisense γPNA. The toehold nucleation and strand displacement reaction is initiated through sense γPNA (black) injection. Branch migration phenomena (unresolvable by SPR) leads to complete strand displacement, resulting in overall mass loss from the chip. The ratio of loading versus loss due to displacement is taken as the percent displacement.

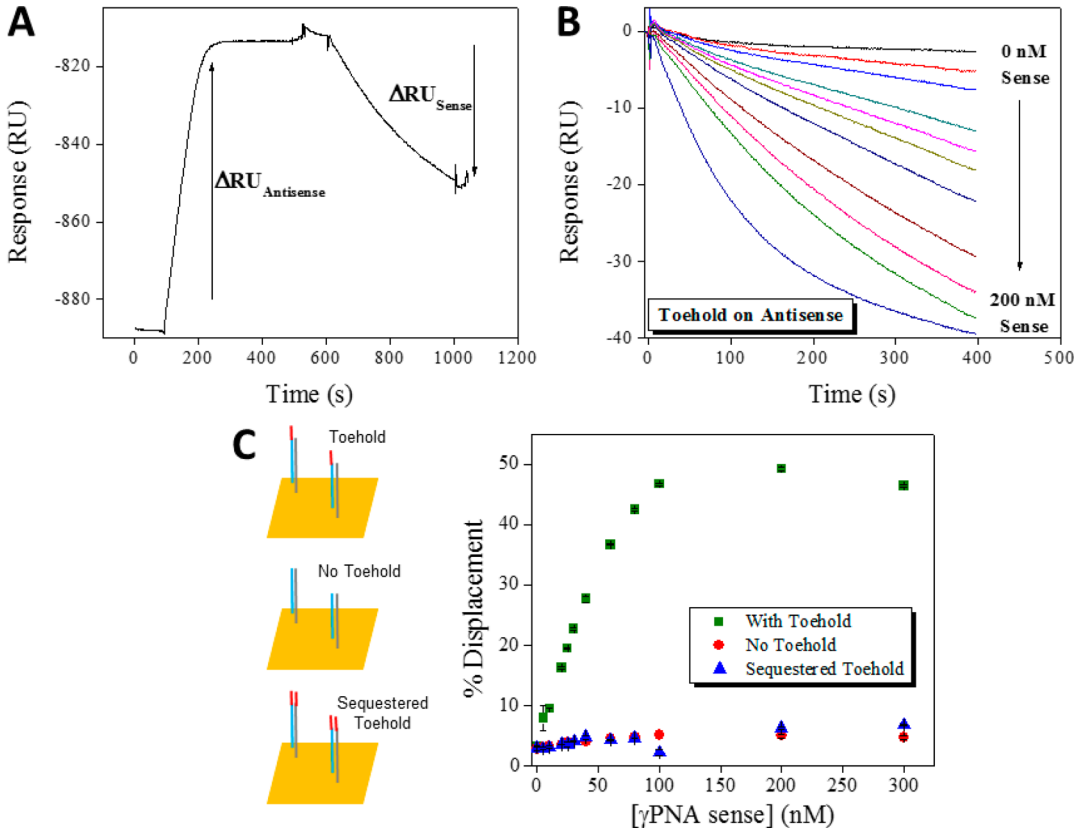

Figure 4. Surface plasmon characterization of γPNA displacement from complementary DNA. (A) Calculation of percent displacement. The response unit change due to sense γPNA dissociation (ΔRU Sense) is divided by initially hybridized antisense γPNA (ΔRU Antisense). The experiments were conducted so that ΔRU antisense is constant for all runs. (B) Dissociation of antisense γPNA through increasing sense γPNA concentrations over time. Every SPR run used a constant antisense concentration of 20 nM, which was injected onto the SPR chip to hybridize the immobilized target DNA. Sense γPNA was then titrated (0–200 nM), to allow for displacement of the antisense γPNA from the chip. (C) Various antisense conditions were considered including: toehold, no toehold, and sequestered toehold (left). The total displacement of the achieved by the various conditions is shown (right). (All data in panel C is presented as average of $n = 2 \pm$ SD).

mRNA (1 h at 37 °C in 79 mM K^+ buffer). The sense γPNA was then introduced and allowed to interact with the antisense γPNA-mRNA complex over time. The total mixture (mRNA, antisense/sense γPNA) was subsequently added to the Rabbit Reticulocye Lysate (RRL) and luciferase bioluminescence was measured using a TECAN plate reader after 90 min of translation. Following this approach, γPNA translation recovery was observed across a range of sense γPNA incubation times at equimolar sense–antisense (100 nM) concentrations in a time-dependent fashion (Figure 5A), with ca. 20% translation recovery observed in 1 h, increasing to ca. 75% recovery in 3 h.

DOI: 10.1021/jacs.5b05351
J. Am. Chem. Soc. 2015, 137, 10268–10275

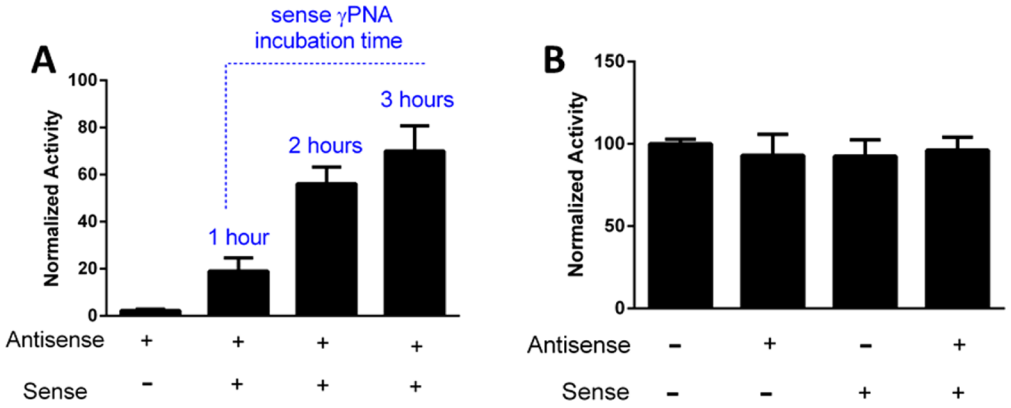

Figure 5. Time dependent translation recovery via γPNA−γPNA displacement. (A) The amount of luciferase translation recovery observed was directly related to the sense γPNA incubation times. At 3-h sense γPNA translation recovery approached ∼75% activity opposed to only ∼20% when 1-h incubations were performed. Equimolar (100 nM) antisense γPNA/sense γPNA was used with 10 nM of target mRNA for all samples (data is plotted as n = 3 average ± SD). (B) When the antisense γPNA alone or sense alone or both were incubated (1 h at 37 °C) against an orthogonal mRNA transcript (scrambled antisense γPNA target site), we observed insignificant (p > 0.05) luciferase knockdown ([γPNA] = 100 nM, [mRNA] = 10 nM) (data is plotted as n = 3 average ± SD).

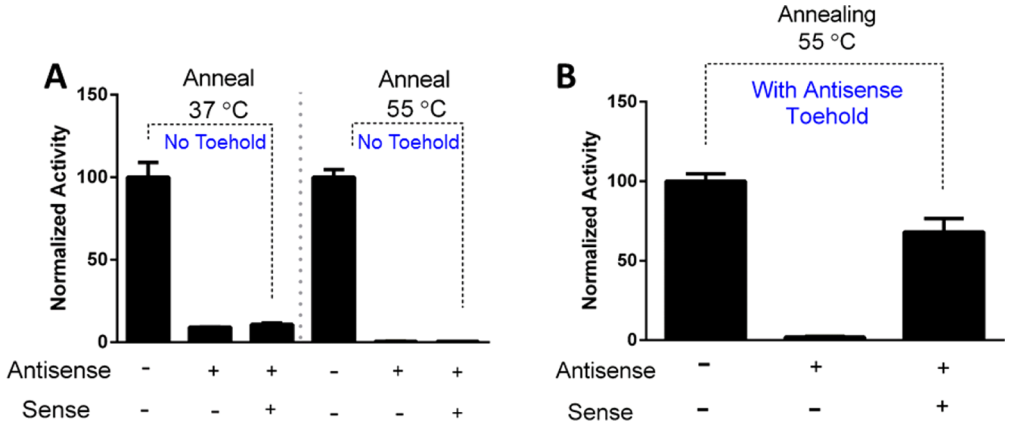

Figure 6. An antisense toehold is required to reverse γPNA-mediated translation inhibition. (A) The absence of the antisense γPNA toehold domain eliminates any observed sense γPNA translation recovery (2-h sense incubation [γPNA] = 100 nM, n = 3); however, the toehold loss does not affect the antisense potency, see (+,-) bar. Additionally, the loss of the antisense γPNA toehold eliminates any observed translation recovery regardless of applying an elevated sense γPNA incubation temperature (55 °C) see (+,+) bar (data is plotted as n = 3 average ± SD). (B) When the antisense γPNA toehold is available, applying an elevated temperature (55 °C) sense γPNA incubation yields high values of translational recovery (∼70%) compared to the knockdown (p = 0.0002) (data is plotted as n = 3 average ± SD).

The time dependence almost certainly indicates that our probe-driven reversibility has kinetic limitations. To ensure that the antisense γPNA does not knockdown an orthogonal luciferase, we incubated the toehold extended antisense γPNA at the high end of the dose range (100 nM) against a luciferase (10 nM mRNA) transcript with a scrambled target-binding site. We observed no knockdown of the luciferase expressed from the orthogonal transcript when compared to the 0 nM antisense γPNA control (Figure 5B). These results reflect the high degree of affinity and specificity antisense γPNA has for the target sequence of the transcript. Lastly, to show that the sense γPNA/mRNA interaction (no antisense present) does not cause elevated expression, the sense γPNA was incubated with the mRNA (100 nM sense, 2-h incubation, 10 nM mRNA) and then added to the RRL. Again, the sense γPNA showed no effect on protein expression levels when compared to the 0 nM γPNA control (Figure 5B).

The reversibility of an antisense γPNA that lacks the toehold domain was evaluated to determine if the increased γPNA−γPNA duplex stability alone was sufficient to reactivate translation. Initially, we annealed the "toehold-less" antisense γPNA to the luciferase mRNA at 37 °C. Next, we introduced the sense γPNA to the annealed mRNA/antisense γPNA and let the ternary mixture incubate for 2 h before adding the entire mixture to the RRL for translation. While the antisense-driven luciferase knockdown was conserved without the presence of a toehold domain, the sense-mediated reversibility was abolished completely (Figure 6A), indicating the importance of the antisense toehold as a nucleation site required to recover gene translation. Furthermore, similar results were observed even at elevated temperatures (55 °C) applied over a 2-h sense incubation time. Applying the same reaction conditions (sense incubation at 55 °C) to a toehold-containing antisense γPNA showed increased recovery of translation (Figure 6B) when compared to recovery values obtained at 37 °C sense incubation (70% versus 55%).

An alternative to regulation of translation by exogenous sense γPNA is to utilize expressible RNA (e.g., miRNA, mRNA, or lncRNA) or exogenously supplied RNA (i.e., siRNA). Therefore, a sense RNA was tested for its ability to displace the

DOI: 10.1021/jacs.5b05351
J. Am. Chem. Soc. 2015, 137, 10268−10275

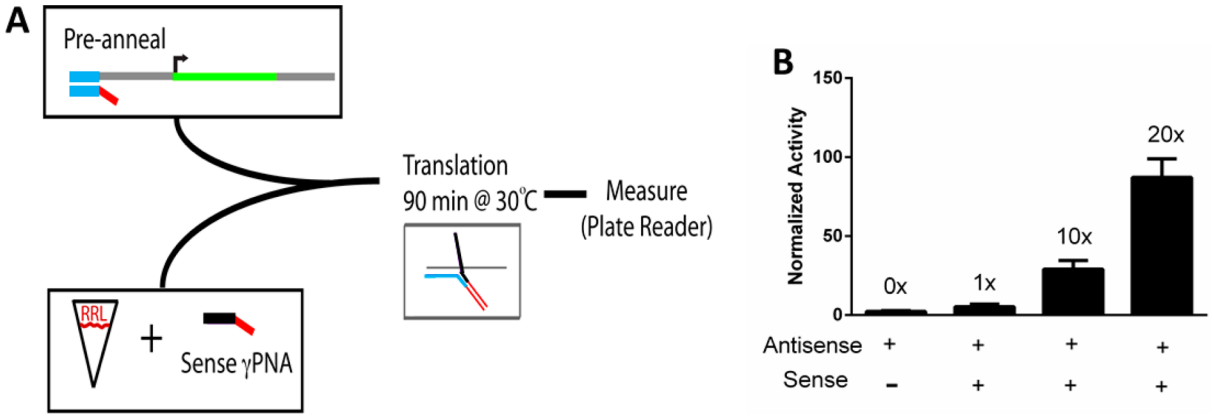

Figure 7. (A) Reversible translation through addition of sense γPNA (1−20×) into rabbit reticulocyte lysate (RRL). The antisense γPNA (100 nM) is preannealed (1 h at 37 °C) to the mRNA prior to the introduction into the RRL. The translation reaction then proceeds for 90 min at 30 °C. Translation recovery as a function of sense γPNA concentration (N = 3 for all concentrations). (B) 0× represents 100 nM antisense γPNA (+,-), with no added sense γPNA. Significant ($p < 0.05$) translational recovery is seen at 10-fold and 20-fold sense concentration compared to antisense (100 nM) alone (~98% knockdown) (data is plotted as n = 3 average ± SD).

antisense γPNA (Figure S7A). The sense RNA (200 nM) was incubated with preannealed antisense γPNA/mRNA sample over the course of 2 h. A 2-fold excess (200 nM) of sense RNA was required to obtain ~30% translation recovery (Figure S7B). This differs from the sense γPNA experiments where 2-h equimolar sense−antisense (100 nM) incubations gave ~55% recovery. Furthermore, sense RNA concentrations that were 10-fold higher (1 μM sense) than antisense γPNA yielded similar translation recovery results to 200 nM sense RNA. Additionally, we tested sense RNA driven-displacement on the SPR (Figures S5 and s6); however, we did not observe antisense γPNA displacement, which could be due to nonoptimized toehold design (e.g., length, sequence, etc.) or the much shorter time scale of the SPR experiment, where the sense RNA only has 400 s during which to displace the antisense γPNA versus a 2 h incubation prior to beginning in vitro translation.

To demonstrate translational control under physiological translation conditions, we tested sense γPNA reversal directly in a functional translation lysate system (Figure 7A). The sense γPNA was added at various concentrations to the RRL solution. These lysates were then charged with the antisense γPNA/mRNA complex (100 nM of antisense, 10 nM mRNA), and translation proceeded for 90 min. As expected, when no sense γPNA is present, ~98% of luciferase activity is blocked by the antisense strand (Figure 7B). Translation of luciferase is restored in a concentration-dependent manner, ultimately achieving ~90% recovery at a 20-fold (20×) excess of sense γPNA (Figure 7B). Considering the antisense reversal in lysates, this suggests that such control may be possible in native physiological environments (e.g., cells), provided the excess sense strand does not exert significant off-target effects.

DISCUSSION

Reversible and selective translation control will provide a tool that is useful in the study of fundamental biological processes as well as in synthetic biology. Here, we demonstrated reversible translational regulation of a luciferase reporter in a cell-free system using γPNA strand displacement driven by toehold recognition.[33] Translation blocked by an antisense γPNA targeted to the 5′-terminus of the mRNA could be restored through addition of either a sense γPNA or a synthetic RNA designed to be fully complementary to the antisense γPNA. The latter result opens the door toward using endogenous sense molecules (e.g., miRNA) to reverse translational inhibition by an antisense γPNA, although further optimization of the toehold is needed to enhance the potency of reversal by RNA. In addition, successful demonstration of PNA as an inhibitor of transcription,[34] splicing[14,15,22] and miRNA function[21,22] suggests that our γPNA-based approach can be extended to allow reversible control over other steps in gene expression.

In addition to the luciferase reporter experiments, we developed a new SPR method to monitor strand displacement reactions in real time without the need for fluorescent labels.[35] This method should be useful for studying the kinetics of strand displacement for any other natural or synthetic nucleic acid. With growing interest in nucleic acid−based computing, SPR provides an attractive platform on which to study hybridization reactions in a label-free, automated, medium-throughput manner.

We anticipate that the γPNA displacement method may be useful in more elaborate cell-free experiments that include multiple gene targets, which are to be controlled discretely and independently, or to exert control over multiple open reading frames on a single transcript. Nevertheless, the simultaneous regulation of multiple genes will require careful sequence design of the γPNA system in order to limit off-target binding and maximize translation activation. Future improvements upon the γPNA design, for instance by altering toehold sequence and length, or by increasing probe affinities by chemical modification, may lead to enhanced toehold nucleation and subsequent displacement in these types of reactions.

The next logical step in this work is to demonstrate reversible antisense effects in cell culture, which will require effective delivery of γPNAs into cells. Cell-penetrating peptides,[36−38] cationic side chain modifications[25,29,39,40] or small molecule conjugates[41] have all been used to deliver PNAs into cells. In addition, a recent paper reported site-specific genome editing in vivo by γPNA delivered via a polymeric nanoparticle vehicle.[42] A similar nanoparticle formulation could be integrated with our technology to achieve intracellular translation recovery. In practice, this would involve delivering the antisense and sense

DOI: 10.1021/jacs.5b05351
J. Am. Chem. Soc. 2015, 137, 10268−10275

γPNAs in separate transfections. Alternatively, a single nanoparticle bolus that delivers both γPNAs simultaneously could be used if the sense γPNA is prevented from hybridizing to the antisense γPNA, e.g., through introduction of a photoreleasable caging group.[43]

Another concern with moving our reversible translation inhibition to a cellular context is the possibility of off-target binding due to the exceptionally high affinity of γPNA,[24] which could lead to weaker antisense inhibition of the targeted mRNA and/or slower, less potent reversal due to competitive hybridization of one or both γPNAs to unintended sites. However, designing structure into the γPNAs, for example, in the form of a hairpin[44] or competitor strand,[45] could limit such off-target binding while preserving sufficient affinity to drive the key γPNA−γPNA hybridization reaction.

Finally, it could be anticipated that the cellular mRNA surveillance pathways would interfere with our approach by degrading the antisense-targeted transcript before the sense γPNA could be introduced. However, the activation of nonsense-mediated decay (NMD), nonstop-mediated decay (NSD), and no-go decay (NGD) mechanisms are dependent on the presence of a transcript-docked ribosome.[46] In the work presented here, we selected an mRNA target site (terminal 5′-UTR) that prevents 5′-UTR eukaryotic ribosomal initiation. Under this γPNA targeting strategy, we anticipate that little mRNA will be lost due to ribosome-dependent degradation pathways. Similarly, RNaseH-mediated mRNA degradation is unlikely to occur due to the unnatural structure of γPNA. Thus, it should be possible, within cell culture, to trap a transcript using an antisense γPNA and then release it for translation at some later time through addition of the corresponding sense γPNA.

MATERIALS AND METHODS

(γ)PNA Synthesis, Purification, And Characterization. PNA oligomers were synthesized and purified using common protocols. Mass characterization was conducted by MALDI-TOF, and subsequently analyzed for purity by reverse phase HPLC. γPNA oligomers were obtained from PNA Innovations.

Luciferase Plasmids for T7 RNA Polymerase Generation of RNA and in Vitro Protein Synthesis in a Rabbit Reticulocyte Lysate. The T7 Luciferase Control Plasmid, Promega part number L482A, was modified to remove alternate start codons, add the CMV transcription start sequence, a restriction site upstream of the Kozak-ATG and a restriction site at the start codon to enable luciferases to be inserted. The Promega plasmid was digested with BamHI and SacI and the Gaussia luciferase was ligated into the Promega vector. This also introduced an NcoI site at the start codon. The firefly luciferase was PCR amplified, digested, and ligated into NcoI and SacI digested vector.

NcoFFlucF 5′-TATATACCATGGAAGACGCCAAAAACATAAA-GAAAGG-3′

SacFFlucR 5′-TATATAGAGCTCGCCCCCTCGG-3′

This plasmid was then digested with HindIII and BamHI and annealed oligos were ligated to introduce an NheI site and CMV transcription start sequence.

HindCMVtransF 5-AGCTTTCAGATCCGCTAGCGCTA-CCGGG

BamCMVtransR 5′-GATCCCCGGTAGCGCTAGCGGA-TCTGAA

The firefly luciferase plasmid has the T7 promoter, CMV transcription start sequence and restriction sites, HindIII, NheI, BamHI and NcoI at the start codon. There is a SacI site 66 bases from the stop codon and a 30 base polyA sequence following the SacI site.

PCR Amplification of the Firefly Luciferase Plasmid. The firefly plasmid was digested (linearized) using an ApaL1 restriction site located downstream of the encoded polyA tail sequence. The linearized product was purified using the Thermo Scientific GeneJET Gel Extraction Kit protocol. The DNA was then PCR amplified using the NEB PCR Protocol for Phusion High-Fidelity DNA Polymerase (cycled 35 times, PCR program 98 °C, 2 min; 98 °C, 10 s; 45 °C, 15 s; 72 °C, 2 min; 72 °C, 1 min; hold at 4 °C).

Primer design: T7 transcription site 5′-TACGACTCACTATA-GGG-3′

3′poly A tail site 5′-TTTTTTTTTTTTTTTTTTTTTTTT-TTTTTT-3′

The products were purified using the Thermo Scientific Gel Extraction Kit protocol and verified using agarose gel electrophoresis (1.8 kB).

Transcription Reaction and Purification. The transcription reaction followed the Thermo Scientific conventional transcription protocol (50 μL final volume) and consistently gave high RNA product yield (~2.5 μM, determined via NanoDrop spectrophotometer). The transcription reaction was conducted at 37 °C for 2 h. The transcription products were purified using the Thermo Scientific GeneJET RNA Cleanup and Concentration Micro Kit and concentration was measured using a NanoDrop spectrophotometer.

γPNA/mRNA Annealing. The γPNA and RNA were annealed together in the presence of 79 mM potassium chloride (designed to match the K^+ concentration in the rabbit reticulocyte lysate, RRL Promega) and DEPC-treated water. The RNA concentration for all translation experiments is set at 10 nM in the final translation reaction. The probe concentration varies depending on the desired final concentration of probe. The initial antisense probe is annealed at 37 °C for 1 h. In the case of the reversible translation experiments, an additional preincubation time (1−3 h) is given for sense γPNA displacement at 37 °C being careful to maintain the incubation salt concentration (79 mM).

Translation Conditions and Luciferase Readout. The translation reaction was conducted using the Promega Luciferase Assay System (E1500) (rabbit reticulocyte lysate). The PNA concentration is determined by considering the 50 μL final translation reaction volume. The translation reaction is conducted at 37 °C for 2 h. Immediately after, the samples are stored in ice to quench any further protein synthesis. Following the Promega Rabbit Reticulocye Lysate System technical manual, 5 μL of lysate solution is mixed into 50 μL of Promega Luciferase Assay Reagent (E1483) added to a Thermo Scientific Nunc 96 well plate (flat white). The bioluminescence reading was collected on a TECAN Infinite M1000 plate reader.

Surface Plasmon Resonance (SPR). All SPR experiments were performed on a Biacore T100 instrument (GE Healthcare) equipped with a four-channel sensor chip. The commercially available chip is coated with a carboxylmethyl dextran matrix that allows further functionalization with streptavidin via a standard NHS-EDC coupling procedure.[47] Immobilization of streptavidin was continued until 7000 response units (RU) of the protein were captured on each of the four channels (flow cells). The final step of the sensor design involved noncovalent capture of the 5′-biotinylated DNA targets (~150 RU) on the respective flow cells bearing immobilized streptavidin.

Each experiment was preceded by injection of a solution containing 20 nM of the antisense γPNA oligomer for 400 s (flow rate = 30 μL/min). A dissociation time of 1 s was incorporated after the injection to allow for diffusion of unbound antisense oligomers from the sensor surface. The subsequent displacement assay was then performed by injecting a solution containing a fixed concentration of either the sense γPNA or RNA oligomer (flow rate = 30 μL/min) and monitoring the sensor response over 400 s. Each displacement cycle was ended by introducing a pulse of a regeneration cocktail (1 M NaCl, 10 mM NaOH) for 30 s at a flow rate of 50 μL/min. The aforementioned cocktail serves to release any residual antisense/sense oligomers and is followed by a buffer injection (150 s, flow rate = 30 μL/min) to reestablish a baseline prior to the next displacement cycle.

The attenuation in response units following introduction of the sense oligomer was taken as evidence of displacement of the antisense γPNA from the sensor surface. Therefore, we established a quantitative estimate of the displacement reaction by the ratio of signal attenuation

DOI: 10.1021/jacs.5b05351
J. Am. Chem. Soc. 2015, 137, 10268−10275

upon introduction of the sense γPNA, ΔRU (sense), to enhancement upon introduction of the complementary antisense γPNA, ΔRU (antisense) eq 1.

$$\% \text{ Displacement} = \frac{\Delta RU \text{ (sense)}}{\Delta RU \text{ (antisense)}} \times 100 \quad (1)$$

■ ASSOCIATED CONTENT

Supporting Information

The Supporting Information is available free of charge on the ACS Publications website at DOI: 10.1021/jacs.5b05351.

In vitro translation results for antisense PNAs and RNA, control experiments for SPR displacement assays (PDF)

■ AUTHOR INFORMATION

Corresponding Authors

*army@cmu.edu

*bruchez@cmu.edu

Notes

The authors declare the following competing financial interest(s): One of the authors (Bruce Armitage) has a potential competing financial interest associated with this work. He holds equity in PNA Innovations, Inc., which is commercializing PNA technology invented at Carnegie Mellon University.

■ ACKNOWLEDGMENTS

The authors thank Prof. Danith Ly for helpful discussions and the David Scaife Family Charitable Foundation for financial support of this research (Award 141RA01). SPR instrumentation was purchased with support from NSF MRI award 0821296.

■ REFERENCES

(1) Suess, B.; Fink, B.; Berens, C.; Stentz, R.; Hillen, W. *Nucleic Acids Res.* **2004**, *32*, 1610−1614.

(2) Mutalik, V. K.; Guimaraes, J. C.; Cambray, G.; Lam, C.; Christoffersen, M. J.; Mai, Q. A.; Tran, A. B.; Paull, M.; Keasling, J. D.; Arkin, A. P.; Endy, D. *Nat. Methods* **2013**, *10*, 354−360.

(3) Valencia-Sanchez, M. A.; Liu, J. D.; Hannon, G. J.; Parker, R. *Genes Dev.* **2006**, *20*, 515−524.

(4) Hochrein, L. M.; Schwarzkopf, M.; Shahgholi, M.; Yin, P.; Pierce, N. A. *J. Am. Chem. Soc.* **2013**, *135*, 17322−17330.

(5) Isaacs, F. J.; Dwyer, D. J.; Ding, C. M.; Pervouchine, D. D.; Cantor, C. R.; Collins, J. J. *Nat. Biotechnol.* **2004**, *22*, 841−847.

(6) Green, A. A.; Silver, P. A.; Collins, J. J.; Yin, P. *Cell* **2014**, *159*, 925−939.

(7) Young, D. D.; Lively, M. O.; Deiters, A. *J. Am. Chem. Soc.* **2010**, *132*, 6183−6193.

(8) Nielsen, P. E.; Egholm, M.; Berg, R. H.; Buchardt, O. *Science* **1991**, *254*, 1497−1500.

(9) Egholm, M.; Buchardt, O.; Christensen, L.; Behrens, C.; Freier, S. M.; Driver, D. A.; Berg, R. H.; Kim, S. K.; Nordén, B.; Nielsen, P. E. *Nature* **1993**, *365*, 566−568.

(10) Nielsen, P. E. *Curr. Pharm. Des.* **2010**, *16*, 3118−3123.

(11) Liu, B.; Han, Y.; Ferdous, A.; Corey, D. R.; Kodadek, T. *Chem. Biol.* **2003**, *10*, 909−916.

(12) Møllegaard, N. E.; Buchardt, O.; Egholm, M.; Nielsen, P. E. *Proc. Natl. Acad. Sci. U. S. A.* **1994**, *91*, 3892−3895.

(13) Janowski, B. A.; Kaihatsu, K.; Huffman, K. E.; Schwartz, J. C.; Ram, R.; Hardy, D.; Mendelson, C. R.; Corey, D. R. *Nat. Chem. Biol.* **2005**, *1*, 210−215.

(14) Sazani, P.; Gemignani, F.; Kang, S.-H.; Maier, M. A.; Manoharan, M.; Persmark, M.; Bortner, D.; Kole, R. *Nat. Biotechnol.* **2002**, *20*, 1228−1233.

(15) Ivanova, G. D.; Arzumanov, A.; Abes, R.; Yin, H.; Wood, M. J. A.; Lebleu, B.; Gait, M. J. *Nucleic Acids Res.* **2008**, *36*, 6418−6428.

(16) Yin, H.; Lu, Q.; Wood, M. *Mol. Ther.* **2008**, *16*, 38−45.

(17) Bai, H.; You, Y.; Yan, H.; Meng, J.; Xue, X.; Hou, Z.; Zhou, Y.; Ma, X.; Sang, G.; Luo, X. *Biomaterials* **2012**, *33*, 659−667.

(18) Doyle, D. F.; Braasch, D. A.; Simmons, C. G.; Janowski, B. A.; Corey, D. R. *Biochemistry* **2001**, *40*, 53−64.

(19) Kaihatsu, K.; Huffman, K. E.; Corey, D. R. *Biochemistry* **2004**, *43*, 14340−14347.

(20) Knudsen, H.; Nielsen, P. E. *Nucleic Acids Res.* **1996**, *24*, 494−500.

(21) Torres, A. G.; Fabani, M. M.; Vigorito, E.; Williams, D.; Al-Obaidi, N.; Wojciechowski, F.; Hudson, R.; Seitz, O.; Gait, M. J. *Nucleic Acids Res.* **2012**, *40*, 2152−2167.

(22) Cheng, C. J.; Bahal, R.; Babar, I. A.; Pincus, Z.; Barrera, F.; Liu, C.; Svoronos, A.; Braddock, D. T.; Glazer, P. M.; Engelman, D. M.; Saltzman, W. M.; Slack, F. J. *Nature* **2015**, *518*, 107−110.

(23) Dragulescu-Andrasi, A.; Rapireddy, S.; Frezza, B. M.; Gayathri, C.; Gil, R. R.; Ly, D. H. *J. Am. Chem. Soc.* **2006**, *128*, 10258−10267.

(24) Sahu, B.; Sacui, I.; Rapireddy, S.; Zanotti, K. J.; Bahal, R.; Armitage, B. A.; Ly, D. H. *J. Org. Chem.* **2011**, *76*, 5614−5627.

(25) Delgado, E.; Bahal, R.; Yang, J.; Lee, J. M.; Ly, D. H.; Monga, S. P. *Curr. Cancer Drug Targets* **2013**, *13*, 867−878.

(26) Sacui, I.; Hsieh, W.-C.; Manna, A.; Sahu, B.; Ly, D. H. *J. Am. Chem. Soc.* **2015**, *137*, 8603−8610.

(27) Demidov, V. V.; Potaman, V. N.; Frank-Kamanetskii, M. D.; Egholm, M.; Buchardt, O.; Sönnichsen, S. H.; Nielsen, P. E. *Biochem. Pharmacol.* **1994**, *48*, 1310−1313.

(28) Good, L.; Awasthi, S. K.; Dryselius, R.; Larsson, O.; Nielsen, P. E. *Nat. Biotechnol.* **2001**, *19*, 360−364.

(29) Dragulescu-Andrasi, A.; Rapireddy, S.; He, G.; Bhattacharya, B.; Hyldig-Nielsen, J. J.; Zon, G.; Ly, D. H. *J. Am. Chem. Soc.* **2006**, *128*, 16104−16112.

(30) Kozak, M. *Nucleic Acids Res.* **1987**, *15*, 8125−8148.

(31) Jackson, R. J.; Hellen, C. U.; Pestova, T. V. *Nat. Rev. Mol. Cell Biol.* **2010**, *11*, 113−127.

(32) Zhang, D. Y.; Winfree, E. *J. Am. Chem. Soc.* **2009**, *131*, 17303−17314.

(33) Srinivas, N.; Ouldridge, T. E.; Sulc, P.; Schaeffer, J. M.; Yurke, B.; Louis, A. A.; Doye, J. P.; Winfree, E. *Nucleic Acids Res.* **2013**, *41*, 10641−10658.

(34) Hu, J.; Corey, D. R. *Biochemistry* **2007**, *46*, 7581−7589.

(35) Chang, A. L.; McKeague, M.; Liang, J. C.; Smolke, C. D. *Anal. Chem.* **2014**, *86*, 3273−3278.

(36) Koppelhus, U.; Nielsen, P. E. *Adv. Drug Delivery Rev.* **2003**, *55*, 267−280.

(37) Abes, S.; Ivanova, G. D.; Abes, R.; Arzumanov, A. A.; Williams, D.; Owen, D.; Lebleu, B.; Gait, M. J. *Methods Mol. Biol.* **2009**, *480*, 85−99.

(38) Deuss, P. J.; Arzumanov, A. A.; Williams, D. L.; Gait, M. J. *Org. Biomol. Chem.* **2013**, *11*, 7621−7630.

(39) Zhou, P.; Wang, M.; Du, L.; Fisher, G. W.; Waggoner, A.; Ly, D. H. *J. Am. Chem. Soc.* **2003**, *125*, 6878−6879.

(40) Achim, C.; Armitage, B. A.; Ly, D. H.; Schneider, J. W. *Wiley Encyclopedia of Chemical Biology* **2009**, *3*, 588−597.

(41) Shiraishi, T.; Nielsen, P. E. *Bioconjugate Chem.* **2012**, *23*, 196−202.

(42) Bahal, R.; Quijano, E.; McNeer, N. A.; Liu, Y.; Bhunia, D. C.; Lopez-Giraldez, F.; Fields, R. J.; Saltzman, W. M.; Ly, D. H.; Glazer, P. M. *Curr. Gene Ther.* **2014**, *14*, 331−342.

(43) Liu, Q.; Deiters, A. *Acc. Chem. Res.* **2014**, *47*, 45−55.

(44) Bonnet, G.; Tyagi, S.; Libchaber, A.; Kramer, F. R. *Proc. Natl. Acad. Sci. U. S. A.* **1999**, *96*, 6171−6176.

(45) Zhang, D. Y.; Chen, S. X.; Yin, P. *Nat. Chem.* **2012**, *4*, 208−214.

(46) Schweingruber, C.; Rufener, S. C.; Zund, D.; Yamashita, A.; Muhlemann, O. *Biochim. Biophys. Acta, Gene Regul. Mech.* **2013**, *1829*, 612−623.

(47) Nguyen, B.; Tanious, F. A.; Wilson, W. D. *Methods* **2007**, *42*, 150−161.

DOI: 10.1021/jacs.5b05351
J. Am. Chem. Soc. 2015, 137, 10268−10275